Adaptive Urban Traffic Signal Control for Multiple Intersections: An LQR Approach

Jiho Park[1], Tong Liu[1], Chieh Wang[2], Andy Berres[2], Joseph Severino[3], Juliette Ugirumurera[3], Airton G. Kohls[4], Hong Wang[2], Jibonananda Sanyal[2] and Zhong-Ping Jiang[1]

***Abstract*—Traffic congestion leads to severe problems especially in urban traffic networks. It increases the chance of accidents, energy waste, and social costs. In order to address these problems, an adaptive linear quadratic regulator (LQR) approach is developed for traffic signal control at multiple intersections in an urban area. The proposed method controls the green time of the traffic signals to reduce traffic congestion and smooth traffic flow. Real-world data from vision-based traffic sensors are used to build the traffic network model, which mimics the real-world traffic behavior. In addition, the proposed control utilizes recursive least square parameter estimation, which is capable of tracking dynamic changes in traffic conditions. Simulation of Urban MObility (SUMO) is used to analyze the efficacy of the proposed method. Results of the simulation show that the proposed method outperforms pretimed control in various aspects.**

***Index Terms*—Traffic signal control, GRIDSMART camera, adaptive LQR control, recursive least square, model predictive control (MPC), SUMO simulation**

I. Introduction

As the mass production of vehicles became a reality in the early 20th century, there has been a continuous increase in vehicle numbers throughout the United States. The number of vehicles registered in the United States was 279.1 million in 2018 [1]. At the same time, the number of people living in urban areas have also increased. Among the 7.7 billion people living on Earth as of 2019, more than half live in urban areas. As of 2050, the proportion of people living in urban areas is expected to reach about two-thirds of the total population [2], [3] in the world. As a result, the increase in vehicle ownership, population, and urbanization has led to significant occurrences in traffic congestion, pollution and waste of energy.

This manuscript has been authored in part by UT-Battelle, LLC, under contract DE-AC05-00OR22725 with the US Department of Energy (DOE). The US government retains and the publisher, by accepting the article for publication, acknowledges that the US government retains a nonexclusive, paid-up, irrevocable, worldwide license to publish or reproduce the published form of this manuscript, or allow others to do so, for US government purposes. DOE will provide public access to these results of federally sponsored research in accordance with the DOE Public Access Plan (http://energy.gov/downloads/doe-public-access-plan).

[1]J. Park, T. Liu and Z.-P. Jiang are with the Control and Networks Lab, Department of Electrical and Computer Engineering, Tandon School of Engineering, New York University, Brooklyn, NY 11201 USA (e-mail: jp5173@nyu.edu; tl3049@nyu.edu; zjiang@nyu.edu).

[2]C. Wang, A. Berres, H. Wang and J. Sanyal are with the Oak Ridge National Laboratory, Oak Ridge, TN 37831 USA (e-mail: cwang@ornl.gov; berresas@ornl.gov; wangh6@ornl.gov; sanyalj@ornl.gov).

[3]J. Severino and J. Ugirumurera are with the National Renewable Energy Laboratory, Golden, CO 80401 USA (e-mail: Joseph.Severino@nrel.gov; juliette.ugirumurera@nrel.gov).

[4]A. G. Kohls is with the Center for Transportation Research, University of Tennessee, Knoxville, TN 37996-2313 USA (e-mail: akohls@utk.edu).

Traffic congestion during rush hours in mega cities significantly impacts commute time of city people [4]. Also it leads to a huge increase in social cost and pollution. There have been many research works which demonstrated the social cost and pollution caused by traffic congestion in urban areas [5]–[8]. Social cost includes travel time costs, excess use of fuel, vehicle operating costs and increase in operating costs by industry and total revenue loss by industry [9]. It is estimated that the annual social cost of congestion from all commute trips in United States will be about 29 billion dollars [10]. This requires smarter control of traffic operation systems so that traffic flows in urban areas can be made as smooth as possible. Indeed, there have been different approaches to reduce the traffic congestion in urban areas. For example, in [11] the authors proposed a method for a dynamic ride-sharing based on "shareability index" to solve large-scale congestion problems. In [12], the authors have demonstrated that controlling the speed limit can reduce bottleneck locations which cause severe traffic congestion at freeways. In [13], Kazi et al. suggested that a reservation-based smart parking system can reduce the traffic congestion as it helps drivers to find the nearest parking area. Finally, Ahmad et al. [14] analyzed the effectiveness of an earliest-deadline-based scheduling that reduces the traffic delay caused by priority vehicles.

Among many approaches, the most practical and implementable solution for reducing traffic congestion is to optimally control traffic signals at intersections. With the recent improvements on reinforcement learning technologies, reinforcement learning based traffic signal control has been developed [15]–[21]. Also, traffic signal control has been proposed which utilizes the data from vehicle to everything (V2X) communication. For example in [22], Kumar et al. demonstrated the autonomous traffic signal control system for smart cities which utilize Internet of Things (IoT) technology. In order to overcome the disadvantages of pretimed operation, traffic responsive control such as actuated and adaptive traffic signal control have been developed. Adaptive traffic signal control methods, whose parameters are adjusted in response to traffic conditions, are more capable of properly responding to changes in traffic conditions. By doing so, traffic congestion can be alleviated and its throughput in the controlled area increases [23]–[25].

In this regard, a novel real-time adaptive traffic signal control for multiple intersections in urban areas is developed in this work. The contribution of this paper is twofold:

Fig. 1. The fisheye view of a GRIDSMART camera. The sensor detects vehicles as they arrive at the intersection. It estimates each vehicle's speed and it tracks vehicles as they move through the intersection to determine their turn directions.

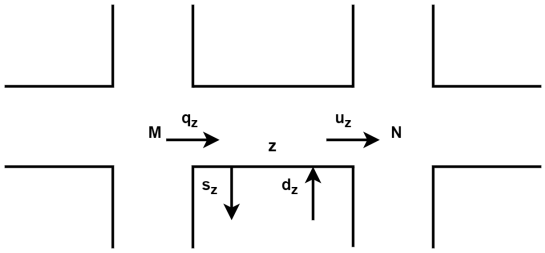

Fig. 2. An urban road links

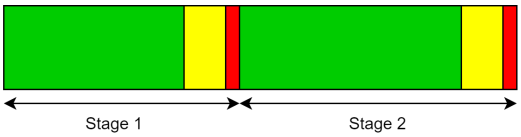

Fig. 3. Stages in intersection

modeling and *control*.

In the *modeling* phase, a *store-and-forward* based model is developed to fit the real-world traffic data in a state-space representation using the well-known recursive least square estimation algorithm. During the *modeling* phase, intersections in downtown Chattanooga, Tennessee, United States, are considered. To build a model which reflects the real-world operation of the intersections, the actual signal timing plan (i.e., minimum and maximum green times, cycle length, offset between intersections, and phase specifications) which is currently used is considered. Real-world traffic data is collected from vision-based traffic sensors, namely the GRIDSMART cameras (Fig. 1). These data are used to fit the model, where the novelty also lies in the use of GRIDSMART camera data to build a traffic flow model.

From a *control* perspective, an adaptive linear quadratic regulator (LQR) controller is used to optimally control each traffic phase's split at each intersection, where *traffic phase* in transportation engineering is defined as the green, change, and clearance intervals in a cycle assigned to specified movement(s) of traffic. The proposed controller calculates the optimal split of each phase from the updated system parameters.

Finally, the *Simulation of Urban MObility* (SUMO) environment, which imitates the real-world traffic flow of intersections in downtown Chattanooga, Tennessee, United States, is utilized to analyze the efficacy of the proposed method.

II. System Modeling

In this paper, we used *store-and-forward* modeling for the urban traffic network system illustrated in [26]. The traffic network can be represented as a directed graph where intersections are considered as nodes and the approaches (or links) are considered as edges, as shown in Fig. 2. In this context, approach z includes several lanes and the vehicles pass through approach z from intersection M to N. Note that the sampling time T is a common multiple of cycle time C for each intersection. For such systems, q_z refers to the inflows to the approach z from upstream intersection M. u_z refers to the outflows from approach z to downstream intersection N. s_z is the exit flow and d_z is the demand flow. By the conservative law of traffic flow, it can be obtained that

$$x_z(k+1) = x_z(k) + T[q_z(k) - s_z(k) + d_z(k) - u_z(k)], \quad (1)$$

where $x_z(k)$ denotes the number of vehicles at time step k. The exit flow can be modeled as

$$s_z(k) = t_{z,0} q_z(k) + \frac{\mu_{z,0}}{T} x_z(k), \quad (2)$$

where $t_{z,0}$ denotes the exit rate from inflow $q_z(k)$ and $\frac{\mu_{z,0}}{T}$ denotes the average exit rate from current state $x_z(k)$ with $\mu_{z,0} \in (0,1)$. Thus (1) can be reformulated as

$$x_z(k+1) = (1-\mu_{z,0}) x_z(k) + T[(1-t_{z,0}) q_z(k) + d_z(k) - u_z(k)] \quad (3)$$

Assuming that there exists a nominal control strategy [27] such that

$$(1-t_{z,0}) q_z^N + d_z^N - u_z^N = 0 \quad (4)$$

holds, the traffic flow dynamics can be further reformulated as

$$\begin{aligned} x_z(k+1) =& (1-\mu_{z,0}) x_z(k) + T[(1-t_{z,0}) \Delta q_z(k) \\ &+ \Delta d_z(k) - \Delta u_z(k)] \end{aligned} \quad (5)$$

where $\Delta q_z(k) = q_z(k) - q_z^N$, $\Delta d_z(k) = d_z(k) - d_z^N$ and $\Delta u_z(k) = u_z(k) - u_z^N$.

Considering an intersection with two stages as depicted in Fig. 3, each stage includes the green, yellow, and red times. The outflow can be controlled via the duration of the green time in the stage. Yellow time and red time can be regarded as fixed constants. Note that *stage* in Fig. 3 corresponds to *traffic phase* in transportation engineering terminology. Duration of stage i at intersection j can be denoted as $g_{j,i}$ and the constraint on cycle time is given by

$$\sum_{i \in F_j} g_{j,i} = C, \text{ for } j = 1, 2, ..., N \quad (6)$$

where F_j stands for the set of available stages for intersection j, N is the number of intersections in the network, and the green time is constrained by

$$g_{j,i,min} \leq g_{j,i} \leq g_{j,i,max}, \text{ for } j = 1, 2, ..., N \text{ and } i \in F_j \tag{7}$$

where $g_{j,i,min}$ and $g_{j,i,max}$ are the minimum and maximum green times for stage i in intersection j, respectively.

As a result, the outflow $u_z(k)$ can be written as

$$u_z(k) = \frac{S_z}{C} \sum_{i \in v_z} g_{N,i}(k) \tag{8}$$

where v_z denotes the stages when approach z has right of way. Similarly, inflow $q_z(k)$ can be expressed as

$$q_z(k) = \sum_{w \in I_M} t_{w,z} u_w(k) = \sum_{w \in I_M} t_{w,z} \frac{S_w(\sum_{i \in v_w} g_{M,i}(k))}{C} \tag{9}$$

where I_M stands for the approaching links for intersection M and $t_{w,z}$ is the turning rate from approach w to approach z. From (8) and (9), it can be obtained that

$$\begin{aligned} x_z(k+1) = (1-\mu_{z,0})x_z(k) + T[(1-t_{z,0}) \\ \sum_{w \in I_M} \frac{t_{w,z} S_w(\sum_{i \in v_w} \Delta g_{M,i}(k)}{C} + \\ \Delta d_z(k) - \frac{S_z(\sum_{i \in v_z} \Delta g_{N,i}(k))}{C}] \end{aligned} \tag{10}$$

where control input $\Delta g_{j,i} = g_{j,i} - g_{j,i}^N$ denotes the control difference with the nominal control $g_{j,i}^N$. Considering all the approaches in the network, the system has a multiple-input and multiple-output (MIMO) state-space representation as follows,

$$x(k+1) = Ax(k) + B\Delta g(k) + T\Delta d(k) \tag{11}$$

where $x(k)$, $\Delta g(k)$, $\Delta d(k)$ are the number of vehicles, control inputs, and demand disturbance for the approaches in the network, respectively. Matrix A is a diagonal matrix with diagonal elements being $1-\mu_{z,0}$ and matrix B includes the connection of intersections, turning rates and saturation flows.

Using (6), the dimension of control inputs can be decreased. For the nominal control $g_{j,i}^N$, we should have the following constraint

$$\sum_{i \in F_j} g_{j,i}^N = C, \tag{12}$$

and we also have

$$\sum_{i \in F_j} \Delta g_{j,i} = 0, \text{for } j = 1, 2, ..., N, \tag{13}$$

Thus, one control input at each intersection can be discarded. For example, if the intersection has only two control inputs $\Delta g_{1,1}$ and $\Delta g_{1,2}$, and $\Delta g_{1,1} + \Delta g_{1,2} = 0$. Then,

$$\begin{bmatrix} b_{11} & b_{12} \\ b_{21} & b_{22} \\ b_{31} & b_{32} \end{bmatrix} \begin{bmatrix} \Delta g_{1,1} \\ \Delta g_{1,2} \end{bmatrix} = \begin{bmatrix} b_{21} - b_{11} \\ b_{22} - b_{21} \\ b_{32} - b_{31} \end{bmatrix} \Delta g_{1,2} \tag{14}$$

where $\Delta g_{1,1}$ has been replaced by $-\Delta g_{1,2}$. For convenience, we will still use (11) as the model where B and $\Delta g(k)$ refer to the matrix and control with reduced dimensions.

III. Controller design

A. The Recursive Least Squares Estimation

The online estimation of A and B matrices based on the real-time data is shown below. Assuming that the disturbance $T\Delta d(k)$ is bounded with $||T\Delta d(k)|| \leq \bar{w}$, then the recursive least squares method with forgetting factor λ can be employed here to identify the unknown parameters. In order to formulate the standard form of recursive least squares, assume that $x(k) \in \mathbb{R}^n$ and by vectorizing both sides of (11), it can be obtained that

$$x(k+1) = ([x(k)^T \otimes I_n]\text{vec}([A\ B]) + Td(k) \tag{15}$$

Using the property of Kronecker product, we have $\text{vec}(AXB) = (B^T \otimes A)\text{vec}(X)$.

Denote $y_{k+1} = x(k+1)$, $\psi_k^T = [x(k)^T\ u(k)^T] \otimes I_n$, $\theta = \text{vec}([A\ B])$ and $w_k = Td(k)$. The algorithm can be summarized as follows:

- Step 0: Initialize forgetting factor $0 < \lambda < 1$, positive definite matrices P_{-1} and T_{-1}, initial estimate $\hat{\theta}_0$ and iteration steps K. Let $k = 0$ and repeat:
- Step 1: $\hat{\theta}_{k+1} = \hat{\theta}_k + P_{k-1}\psi_k D_k^{-1}(y_{k+1} - \psi_k^T \hat{\theta}_k)$ with $D_k = \lambda T + \psi_k^T P_{k-1} \psi_k$
- Step 2: $P_k = \lambda^{-1}(I - P_{k-1}\psi_k D_k^{-1}\psi_k^T)P_{k-1}$
- Step 3: $k := k+1$; If $k > K$, set output as the current estimate $\hat{\theta}_k$, otherwise go to step 1.

To ensure good estimation, the following persistent excitation conditions [28] should be satisfied for the data to be used. This condition says that for some $S \in \mathbb{N}_{\geq 0}$, for all $j \in \mathbb{N}_{\geq 0}$, the following inequality should be satisfied

$$0 < \alpha I \leq \sum_{i=j}^{j+S} \psi_i \psi_i^T \leq \beta I < \infty \tag{16}$$

where α, β are positive constants. This ensures that the estimation error will satisfy

$$||\hat{\theta}_k - \theta|| \leq \gamma_1 \lambda^{k/2} ||\hat{\theta}_0 - \theta|| + \gamma_2 \lambda^{k/2} \bar{w} + \gamma_3 \frac{1-\lambda^{k/2}}{1-\lambda^{1/2}} \bar{w} \tag{17}$$

where θ is the true parameter, γ_1, γ_2, and γ_3 are non-negative constants with γ_3 proportional to $1/\alpha$. As k tends to go infinity, the estimation error can be dramatically decreased by increasing α through collecting rich enough data [29]. Finally, matrices A and B can be extracted through $\hat{\theta}_k$. Initial parameters P_{-1}, T_{-1} and $\hat{\theta}_0$ are known and $\hat{\theta}_k$ is updated by the following optimization problem:

$$\arg\min_{\hat{\theta}_k} \frac{1}{2}\lambda^k ||\hat{\theta}_0 - \hat{\theta}_k||^2_{P_{-1}^{-1}} + \frac{1}{2}\sum_{i=1}^{k} \lambda^{k-i} ||y_i - \psi_{i-1}^T \hat{\theta}_k||^2_{T_{-1}^{-1}} \tag{18}$$

where P_{-1} and T_{-1} refer to the confidence on the initial estimation and new estimation, respectively. These values can be chosen offline from the historical data.

B. Linear Quadratic Regulator

The following LQR problem is considered:

$$\begin{aligned} \min_{u_0,u_1,\dots} \quad & \sum_{k=0}^{\infty} \epsilon x(k)^T Q x(k) + u(k)^T u(k) \\ \text{s.t.} \quad & x(k+1) = Ax(k) + Bu(k) \end{aligned} \tag{19}$$

where $u(k) = \Delta g(k)$; ϵ is a positive constant that can be adjusted; Q is a positive definite matrix whose diagonal elements are $1/x_{z,max}$ as in [27]. The goal of LQR control is to reduce the quadratic cost function which can be done by optimizing the state or input. Besides, it is evident that the eigenvalues of A are within the unit circle of complex plane and (A, B) is stabilizable pair accordingly. This fact can be validated from the fact that when $u(k) = 0$ for $i = 1, 2, ..., x(k)$ does not go to infinity as k increases. Therefore, there exists a unique real symmetric and positive definite matrix P satisfying the following algebraic Riccati Equation (ARE)

$$P = A^T PA - A^T PB(B^T PB + I)^{-1} B^T PA + \epsilon Q \tag{20}$$

This leads to the following optimal control law,

$$u^*(k) = -(B^T PB + I)^{-1} B^T PAx(k) \tag{21}$$

for the linear quadratic regulator problem [30]. In addition, it turns out that ϵ can be adjusted such that the constraints (7) can be strictly satisfied as follows.

Proposition 1. Assuming that the nominal signal plan satisfies

$$g_{j,i,min} < g^N_{j,i} < g_{j,i,max} \tag{22}$$

for $j = 1, 2, ..., N$ and $i \in v(j)$, then given the initial state $x(0)$, there exists a sufficient small ϵ^* such that when $0 < \epsilon < \epsilon^*$, the optimal control law (21) satisfies the constraints (7) for $j = 1, 2, ..., N$.

Proof: Since (A, B) is stabilizable, control law (21) will stabilize the undisturbed system [30], and the original system (11) is input-to-state stable regarding $T\Delta d(k)$ as the input [31]. Thus there exist positive constants β_1 and β_2 such that $||x(k)|| \leq \beta_1 ||x(0)|| + \beta_2 \bar{w}$ for $k = 1, 2, ..., N$. A positive constraint α can be defined as follows,

$$\alpha = \min_{j=1,\dots,N, i \in v(j)} [|g^N_{j,i} - g_{j,i,min}|, |g_{j,i,max} - g^N_{j,i}|] \tag{23}$$

and we need to guarantee $||u^*(k)||_\infty \leq \alpha$ or $||u^*(k)|| \leq \alpha$. It is known that $\lim_{\epsilon \to 0} P(\epsilon) = 0$ [32], combining with the boundedness of $x(k)$, when $\sigma = \frac{\alpha}{||A||||B||(\beta_1 ||x(0)|| + \beta_2 \bar{w})}$, there exists $\epsilon^* > 0$ such that when $\epsilon < \epsilon^*$, $||P(\epsilon)|| < \sigma$ and

$$\begin{aligned} ||u^*(k)|| &\leq ||(B^T PB + I)^{-1}||||B||||P||||A||||x(k)|| \\ &\leq ||B||||P||||A||||x(k)|| < \alpha \end{aligned} \tag{24}$$

for each $k = 1, 2, ...$, which completes the proof.

In the proposed algorithm, coefficient ϵ is adjusted to make sure constraints (7) are satisfied.

C. Model Predictive Control

A finite horizon constrained optimization problem is formulated to obtain a desired controller by explicitly considering the constraints (7). The problem to be solved is therefore as follows,

$$\begin{aligned} \min_{u_0,u_1,\dots,u_K} \quad & \sum_{k=0}^{K} x(k)^T Q x(k) + u(k)^T R u(k) \\ \text{s.t.} \quad & x(k+1) = Ax(k) + Bu(k) \\ & g_{j,i,min} \leq g_{j,i} \leq g_{j,i,max}, \\ & \text{for } j = 1, 2, ..., N \text{ and } i \in F(j) \end{aligned} \tag{25}$$

where K is the planning horizon and Q and R are two real symmetric and positive definite matrices. Considering K states, we have

$$\begin{bmatrix} x(1) \\ x(2) \\ \vdots \\ x(K) \end{bmatrix} = \begin{bmatrix} A \\ A^2 \\ \vdots \\ A^K \end{bmatrix} x(0) + \begin{bmatrix} B & 0 & \dots & 0 \\ AB & B & \dots & 0 \\ \vdots & \vdots & \ddots & \vdots \\ A^{K-1}B & A^{K-2}B & \dots & B \end{bmatrix} \begin{bmatrix} u(0) \\ u(1) \\ \vdots \\ u(k-1) \end{bmatrix} \tag{26}$$

denoted as $X = \bar{A}x_0 + \bar{B}U$, and the cost function

$$\begin{aligned} J(U) &= X^T (I_K \otimes Q) X + U^T (I_K \otimes R) U \\ &= U^T (\bar{B}^T Q_K \bar{B} + R_K) U + 2U^T B^T Q_K \bar{A} x_0 + g(x_0) \end{aligned} \tag{27}$$

where $Q_k = I_k \otimes Q$ and $R_k = I_k \otimes R$, and the Hessian matrix is

$$\nabla^2 J(U) = \bar{B}^T Q_k \bar{B} + R_k > 0 \tag{28}$$

Thus, $J(U)$ is a convex function over the decision variable U, and the constraints (7) can be rewritten as $GU \leq h$ with appropriate matrices G and h, which defines a convex feasible set.

IV. Simulation results

SUMO simulations were conducted to validate our proposed control methods [33]. As shown in Fig. 4, 11 intersections in downtown Chattanooga (Tennessee, the United States) are considered. Among the 11 intersections, 8 intersections have 2 stages, 2 intersections have 3 stages and the remaining 1 intersection has 4 stages. This implies the control input to be $u(k) \in \mathbb{R}^{13}$. Besides, there are 38 links in the intersections which means that $x(k) \in \mathbb{R}^{38}$ accordingly.

One month of historical data (which were collected by the GRIDSMART cameras) of morning rush hours, (i.e., weekdays, 7:00-9:00 AM) including the signal timing plan, vehicle counts and vehicle speeds are used to establish and calibrate the SUMO simulation model. Each intersection's index, name, location (from North to South) and existing pretimed signal plan are shown in Table I, and used as the nominal control input.

After a few iterations, the testing error converges to a small value and the variation of parameters does not change a lot as displayed in Fig. 5 and Fig. 6 which show the mean absolute percentage error (MAPE) compared with other approaches including linear regression and a well-tuned neural network (1 hidden layer with 340 neurons). In Table II, the recursive least squares estimation does not outperform linear regression method since the latter has considered all the data for

Fig. 4. Traffic network in downtown Chattanooga, Tennessee, United States

TABLE I
INTERSECTIONS AND PRETIMED SIGNAL PLANS

Intersection index / name	Configuration		
	Cycle time (sec)	Number of stage	Each stage's time (sec)
1 / Georgia Avenue & E 4th Street	140	4	36, 57, 15, 32
2 / Lindsay Street & E 4th Street	140	2	96, 44
3 / Houston Street & E 4th Street	140	2	115, 25
4 / Georgia Avenue & E 6th Street	70	2	28, 42
5 / Georgia Avenue & McCallie Avenue	140	3	55, 34, 51
6 / Lindsay Street & McCallie Avenue	140	2	99, 41
7 / Houston Street & McCallie Avenue	140	2	102, 38
8 / Georgia Avenue & E 8th Street	70	2	28, 42
9 / Georgia Avenue & E.M.L King Blvd	140	3	47, 36, 57
10 / Lindsay Street & E.M.L King Blvd	140	2	98, 42
11 / Houston Street & E.M.L King Blvd	140	2	107, 33

*Order of intersections begins from North to South

prediction and recursive least squares gives more weights on recent data.

The following three indices are measured to compare the performance of controllers: sum of the number of vehicles at each sampling time, sum of waiting time for all vehicles at each sampling time, sum of the number of stopping vehicles at each sampling time. Simulation is carried out for 7200 (sec) where 9539 vehicles are put into the network during this time. 15% of nominal control's splits are set as the bound in (7). Once the control input exceeds the bound, it is set as

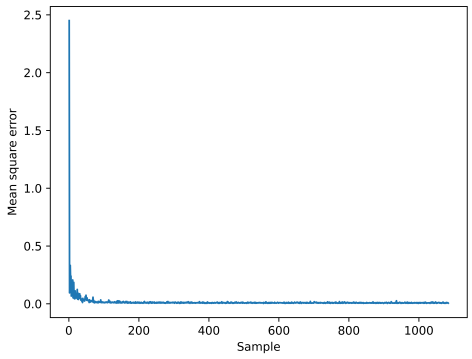

Fig. 5. Convergence of mean square error

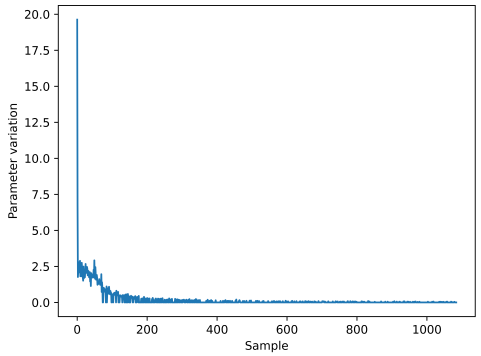

Fig. 6. Variation of parameters

the corresponding bound values. The result for different ϵ is shown in Table III. It can be seen that the proposed adaptive LQR controller outperforms the MPC controller with $K = 3$ and the pretimed controller as given in Table IV. In addition, the adaptive LQR control outperforms pretimed control in that the number of the vehicles at links, waiting time, and the number of stops is reduced by 5.51%, 20.82%, 12.72%, respectively. Also, simulation is carried out for 7200 (sec) and the results are shown in Table V and VI. It can be concluded that the proposed algorithm is not sensitive to the selection of random seeds and outperforms the pretimed controller.

V. CONCLUSION

This paper proposed a novel *store-and-forward* based traffic network modeling and designed an adaptive LQR traffic signal control for multiple intersections in urban traffic networks. The traffic model was developed using the recursive least square estimation which updates system parameters for every iteration. Once the modeling process is performed, an LQR controller is designed that provides optimal control input (i,e., green time of next cycle) to reduce the traffic congestion within the controlled area. SUMO simulation using GRIDSMART real-time data are carried out to demonstrate the capacity of the proposed method, and desired results have been obtained.

TABLE II
MEAN ABSOLUTE PERCENTAGE ERROR (MAPE) FOR DIFFERENT APPROACHES

MAPE (%)	Approaches		
	RLS	*Linear regression*	*Neural network*
Mean value	19.39	17.46	21.05
Maximum value	39.28	31.38	45.74

TABLE III
IMPACT OF CONSTANT (ϵ) ON THE PERFORMANCE INDICES

Performance index	Different values of constant (ϵ)				
	0.33	*0.5*	*0.65*	*1*	*2*
#Violation	0	0	0	1	10
#Vehicles	4839	4809	4807	4812	4832
#Stops	3454	3407	3387	3324	3374
Waiting time (sec)	94752	93228	91747	88659	90375

TABLE IV
PERFORMANCE COMPARISON FOR THREE DIFFERENT METHODS

Type of control	Performance index		
	#Vehs	Waiting time (sec)	#Stops
Adaptive LQR	4677	78402	3107
MPC ($K = 3$)	4877	94464	3460
Pretimed control	4950	99020	3560

TABLE V
SENSITIVITY OF ADAPTIVE LQR CONTROL

Statistics value	Performance index		
	#Vehs	Waiting time (sec)	#Stops
Mean	4707	81026	3154
Standard deviation	28.36	1302	32.25

TABLE VI
SENSITIVITY OF PRETIMED CONTROL

Statistics value	Performance index		
	#Vehs	Waiting time (sec)	#Stops
Mean	4951	99197	3557
Standard deviation	13.80	650	16.47

ACKNOWLEDGMENT

This work is supported partly by the U.S. Department of Energy (DOE), Vehicle Technologies Office, Energy Efficient Mobility Systems (EEMS) Program and partly by the NSF under Grant EPCN-1903781.

REFERENCES

[1] D. L. Bleviss, "Transportation is critical to reducing greenhouse gas emissions in the united states," *Wiley Interdisciplinary Reviews: Energy and Environment*, vol. 10, no. 2, p. e390, 2021.

[2] U. Desa, "World population prospects 2019: Highlights," *New York (US): United Nations Department for Economic and Social Affairs*, vol. 11, no. 1, p. 125, 2019.

[3] A. Azhar, "Don't call time onthe megacity," *The Great Redesign: Frameworks for the Future*, vol. 4, p. 108, 2021.

[4] A. Páez and K. Whalen, "Enjoyment of commute: A comparison of different transportation modes," *Transportation Research Part A: Policy and Practice*, vol. 44, no. 7, pp. 537–549, 2010.

[5] S. Zheyi and J. Wu, "The comparative study on elasticity of traffic congestion delay cost in beijing, shanghai and guangzhou," in *E3S Web of Conferences*, vol. 253. EDP Sciences, 2021.

[6] M. J. Beckmann, "Traffic congestion and what to do about it," *Transportmetrica B: transport dynamics*, vol. 1, no. 1, pp. 103–109, 2013.

[7] L.-z. Mao, X.-l. Zhang, and L.-r. Duan, "Analysis and research of the social cost of traffic congestion in beijing," in *CICTP 2014: Safe, Smart, and Sustainable Multimodal Transportation Systems*, 2014, pp. 2726–2735.

[8] J. M. Thomson, "Reflections on the economics of traffic congestion," *Journal of transport economics and policy*, pp. 93–112, 1998.

[9] R. Arnott and K. Small, "The economics of traffic congestion," *American scientist*, vol. 82, no. 5, pp. 446–455, 1994.

[10] J. Kim, "Estimating the social cost of congestion using the bottleneck model," *Economics of Transportation*, vol. 19, p. 100119, 2019.

[11] N. Alisoltani, L. Leclercq, and M. Zargayouna, "Can dynamic ride-sharing reduce traffic congestion?" *Transportation research part B: methodological*, vol. 145, pp. 212–246, 2021.

[12] Z. Li, P. Liu, C. Xu, H. Duan, and W. Wang, "Reinforcement learning-based variable speed limit control strategy to reduce traffic congestion at freeway recurrent bottlenecks," *IEEE transactions on intelligent transportation systems*, vol. 18, no. 11, pp. 3204–3217, 2017.

[13] S. Kazi, S. Nuzhat, A. Nashrah, and Q. Rameeza, "Smart parking system to reduce traffic congestion," in *2018 International Conference on Smart City and Emerging Technology (ICSCET)*. IEEE, 2018, pp. 1–4.

[14] A. Ahmad, R. Arshad, S. A. Mahmud, G. M. Khan, and H. S. Al-Raweshidy, "Earliest-deadline-based scheduling to reduce urban traffic congestion," *IEEE Transactions on Intelligent Transportation Systems*, vol. 15, no. 4, pp. 1510–1526, 2014.

[15] H. Wei, G. Zheng, H. Yao, and Z. Li, "Intellilight: A reinforcement learning approach for intelligent traffic light control," in *Proceedings of the 24th ACM SIGKDD International Conference on Knowledge Discovery & Data Mining*, 2018, pp. 2496–2505.

[16] X. Liang, X. Du, G. Wang, and Z. Han, "A deep reinforcement learning network for traffic light cycle control," *IEEE Transactions on Vehicular Technology*, vol. 68, no. 2, pp. 1243–1253, 2019.

[17] S. S. Mousavi, M. Schukat, and E. Howley, "Traffic light control using deep policy-gradient and value-function-based reinforcement learning," *IET Intelligent Transport Systems*, vol. 11, no. 7, pp. 417–423, 2017.

[18] D. Garg, M. Chli, and G. Vogiatzis, "Deep reinforcement learning for autonomous traffic light control," in *2018 3rd ieee international conference on intelligent transportation engineering (icite)*. IEEE, 2018, pp. 214–218.

[19] M. Coşkun, A. Baggag, and S. Chawla, "Deep reinforcement learning for traffic light optimization," in *2018 IEEE International Conference on Data Mining Workshops (ICDMW)*. IEEE, 2018, pp. 564–571.

[20] T. Wu, P. Zhou, K. Liu, Y. Yuan, X. Wang, H. Huang, and D. O. Wu, "Multi-agent deep reinforcement learning for urban traffic light control in vehicular networks," *IEEE Transactions on Vehicular Technology*, vol. 69, no. 8, pp. 8243–8256, 2020.

[21] N. Kumar, S. S. Rahman, and N. Dhakad, "Fuzzy inference enabled deep reinforcement learning-based traffic light control for intelligent transportation system," *IEEE Transactions on Intelligent Transportation Systems*, vol. 22, no. 8, pp. 4919–4928, 2020.

[22] S. Suresh Kumar, M. Rajesh Babu, R. Vineeth, S. Varun, A. Sahil, and S. Sharanraj, "Autonomous traffic light control system for smart cities," in *Computing and Network Sustainability*. Springer, 2019, pp. 325–335.

[23] H. Wang, M. Zhu, W. Hong, C. Wang, G. Tao, and Y. Wang, "Optimizing signal timing control for large urban traffic networks using an adaptive linear quadratic regulator control strategy," *IEEE Transactions on Intelligent Transportation Systems*, vol. 23, no. 1, pp. 333–343, 2020.

[24] W. Hong, G. Tao, H. Wang, and C. Wang, "Traffic signal control with adaptive online-learning scheme using multiple-model neural networks," *IEEE transactions on neural networks and learning systems*, 2022.

[25] Q. Wang, J. Severino, H. Sorensen, J. Sanyal, J. Ugirumurera, C. R. Wang, A. Berres, W. Jones, A. Kohls, and R. Paleti, "Deploying a model predictive traffic signal control algorithm – a field deployment case study," *Transportation Research Board (TRB) Annual Meeting*, 2022.

[26] K. Aboudolas, M. Papageorgiou, and E. Kosmatopoulos, "Store-and-forward based methods for the signal control problem in large-scale congested urban road networks," *Transportation Research Part C: Emerging Technologies*, vol. 17, no. 2, pp. 163–174, 2009.

[27] C. Diakaki, M. Papageorgiou, and K. Aboudolas, "A multivariable regulator approach to traffic-responsive network-wide signal control," *Control Engineering Practice*, vol. 10, no. 2, pp. 183–195, 2002.

[28] S. Brüggemann and R. R. Bitmead, "Exponential convergence of recursive least squares with forgetting factor for multiple-output systems," *Automatica*, vol. 124, p. 109389, 2021.

[29] P. A. Ioannou and J. Sun, *Robust adaptive control*. PTR Prentice-Hall Upper Saddle River, NJ, 1996, vol. 1.

[30] G. Hewer, "An iterative technique for the computation of the steady state gains for the discrete optimal regulator," *IEEE Transactions on Automatic Control*, vol. 16, no. 4, pp. 382–384, 1971.

[31] Z.-P. Jiang and Y. Wang, "Input-to-state stability for discrete-time nonlinear systems," *Automatica*, vol. 37, no. 6, pp. 857–869, 2001.

[32] Z. Lin, *Low gain feedback*. Springer, 1999, vol. 240.

[33] P. A. Lopez, M. Behrisch, L. Bieker-Walz, J. Erdmann, Y.-P. Flötteröd, R. Hilbrich, L. Lücken, J. Rummel, P. Wagner, and E. Wießner, "Microscopic traffic simulation using sumo," in *2018 21st international conference on intelligent transportation systems (ITSC)*. IEEE, 2018, pp. 2575–2582.